PREPARATION AND TESTING OF CORROSION- AND SPALLATION-RESISTANT COATINGS

Annual Topical Report

Reporting Period Start Date: October 1, 2012
Reporting Period End Date: September 30, 2013

Project Reporting Period: October 1, 2011 – September 30, 2014

Principal Author: John P. Hurley

Report Issue Date: October 2013
DOE NETL Cooperative Agreement DE-FE0007325
Performance Monitor: Stephen Richardson

Submitting Organization:

Energy & Environmental Research Center
15 North 23rd Street, Stop 9018
Grand Forks, ND 58202-9018

John P. Hurley, Project Manager

October 2013

DISCLAIMER

PREPARATION AND TESTING OF CORROSION- AND SPALLATION-RESISTANT COATINGS

ABSTRACT

This Energy & Environmental Research Center (EERC) project is designed to determine if plating APMT®, a specific highly oxidation-resistant oxide dispersion-strengthened FeCrAl alloy made by Kanthal, onto nickel-based superalloy turbine parts is a viable method for substantially improving the lifetimes and maximum use temperatures of the parts. The method for joining the APMT plate to the superalloys is called evaporative metal bonding and involves placing a thin foil of zinc (Zn) between the plate and the superalloy, clamping them together, and heating in an atmosphere-controlled furnace. Upon heating, the Zn melts and dissolves the oxide skins of the alloys at the bond line, allowing the two alloys to diffuse into each other. The Zn then diffuses through the alloys and evaporates from their surfaces.

Laboratory testing to determine the diffusion rate of Zn through the alloys has been completed. We have found that we were not able to create joints when temperatures much lower than the original temperature of 1214°C are used. Therefore, we limited our diffusion rate measurements to the two hold temperatures used in the procedure: 700° and 1214°C. The diffusivity of zinc in both APMT and CM247LC is quite similar at 700°C. Diffusivity in the APMT appears to be slightly higher, but the midline composition after 30 minutes at this temperature is quite similar. At 1214°C, the situation is very different. The calculated diffusivity of zinc in APMT is approximately 15 times higher than in CM247LC or Rene® 80 (~120 vs. ~8 μm^2/min) at that temperature.

In addition to the diffusion work, the coefficients of thermal expansions were determined for each of the alloys as a function of temperature. This information has been entered into a finite element model using ANSYS so that appropriate force-applying structures can be designed for use in joining structures composed of APMT and the nickel alloys.

Gasifier sampling activities continue to determine what types of trace contaminants may occur in cleaned syngas that could lead to corrosion or deposition in turbines firing coal syngas. The EERC has several pilot-scale gasifiers that are continually used in a variety of test configurations as determined by the needs of the projects that are funding the tests. We are sampling both noncombusted and combusted syngas produced during some of the pilot-scale gasifier tests.

After modifying our sampling procedures to minimize contamination from the oxidizer, we obtained very good filter samples from both syngas and from the combustion products of the syngas blended with natural gas. Scanning electron microscopy analyses showed that the particles captured on the filter from the syngas were typically 0.2 to 0.5 μm in diameter, whereas those captured from the combusted syngas were slightly larger and more spherical. However, the particles were so small that we could not obtain good spectra from them either at the EERC or JEOL America, the maker of the EERC electron microscope systems. Therefore, the EERC applied for and received time on electron microscopes using different signal analyzers at the Oak

Ridge National Laboratory (ORNL) ShaRE User Facility, which is sponsored by the U.S. Department of Energy Scientific User Facilities Division of the Office of Basic Energy Sciences. At ORNL, both x-ray photoelectron spectroscopy (XPS) and Auger electron spectroscopy were performed on the samples because these are surface analyses that analyze electrons emitted from within a few nanometers of the surfaces of the particles and filters. The XPS data show that the particles do not contain any metals and, in fact, have an atomic composition almost identical to that of the polycarbonate filter. We currently believe that this indicates that the particles are primarily soot-based and not formed from volatilization of metals in the fluid-bed gasifier. The data indicate that the soot-based particles are not well burned in the thermal oxidizer, although they are significantly oxidized, nitrided, and sulfidized in the combustor. Ion etching to remove the surfaces of the particles indicates that the oxidation, nitridation, and sulfidation of the particles are primarily surface phenomena.

TABLE OF CONTENTS

LIST OF FIGURES

LIST OF TABLES

PREPARATION AND TESTING OF CORROSION- AND SPALLATION-RESISTANT COATINGS

EXECUTIVE SUMMARY

This Energy & Environmental Research Center (EERC) project was designed to determine if plating APMT®, a specific highly oxidation-resistant oxide dispersion-strengthened FeCrAl alloy made by Kanthal, onto nickel-based superalloy turbine parts is a viable method for substantially improving the lifetimes and maximum use temperatures of the parts, both those with thermal barrier coatings and those without. The superalloys being investigated for protection are CM247LC and Rene® 80. Both are alumina-scale-forming alloys. The method for bonding the APMT plate to the superalloys is called evaporative metal bonding, which involves placing a thin foil of zinc (Zn) between the plate and the superalloy, clamping them together, and heating in an atmosphere-controlled furnace. Upon heating, the Zn melts and dissolves the oxide skins of the alloys at the bond line, allowing the two alloys to diffuse into each other. The Zn then diffuses through the alloys and evaporates from their surfaces.

If successful, the information developed will help move the protection process closer to demonstration testing. In addition, the team will characterize the microcontaminants in combusted higher-hydrogen-content gas. This information will be used to best simulate actual corrosion conditions in a turbine system and can also be used by other researchers studying deposition and gas flow in turbines.

Laboratory testing to determine the diffusion rate of Zn through the alloys has been completed. We have found that we were not able to create joints when temperatures much lower than the original temperature of 1214°C are used. Therefore, we limited our diffusion rate measurements to the two hold temperatures used in the procedure: 700° and 1214°C. The diffusivity of zinc in both APMT and CM247LC is quite similar at 700°C. Diffusivity in the APMT appears to be slightly higher (~4 vs. ~2 μm^2/min), but the midline composition after 30 minutes at this temperature is quite similar. At 1214°C, the situation is very different. Because only about 15 wt% zinc remained at the midline after the low-temperature hold, the absolute difference in compositions between the APMT, CM247LC, and Rene 80 at 1214°C is relatively small. However, the calculated diffusivity of zinc in APMT is approximately 15 times higher than in CM247LC or Rene 80 (~120 vs. ~8 μm^2/min) at 1214°C.

In addition to the diffusion work, the coefficients of thermal expansions were determined for each of the alloys as a function of temperature. This information has been entered into a finite element model using ANSYS so that appropriate force-applying structures can be designed for use in joining structures composed of APMT and the nickel alloys.

In addition to the laboratory testing, gasifier sampling activities continue to determine what types of trace contaminants may occur in cleaned syngas that could lead to corrosion or deposition in turbines firing coal syngas. The EERC has several pilot-scale gasifiers that are continually used in a variety of test configurations as determined by the needs of the projects that are funding the tests. Under the University Turbine System Research (UTSR) Program, we are

sampling both noncombusted and combusted syngas produced during some of the pilot-scale gasifier tests.

The gas and particulate sample is withdrawn nonisokinetically from the source, particulate emissions are collected in the probe and on a heated filter, and gaseous emissions are then collected in aqueous acidic solutions of H_2O_2 and $KMnO_4$, respectively. While filters are analyzed using scanning electron microscopy (SEM), impinger solutions are analyzed using inductively coupled plasma–mass spectrometry.

After modifying our sampling procedures to minimize contamination from the oxidizer, we obtained very good filter samples from both syngas and from the combustion products of the syngas blended with natural gas. SEM analyses showed that the particles captured on the filter from the syngas were typically 0.2 to 0.5 μm in diameter, whereas those captured from the combusted syngas were slightly larger and more spherical. However, the particles were so small that we could not obtain good spectra from them either at the EERC or JEOL America, the maker of the EERC electron microscope systems. Therefore, the EERC applied for and received time on electron microscopes using different signal analyzers at the Oak Ridge National Laboratory (ORNL) ShaRE User Facility, which is sponsored by the U.S. Department of Energy Scientific User Facilities Division of the Office of Basic Energy Sciences. At ORNL, both x-ray photoelectron spectroscopy (XPS) and Auger electron spectroscopy were performed on the samples because these are surface analyses that analyze electrons emitted from within a few nanometers of the surfaces of the particles and filters. In XPS, areas of the filter on which particles reside are analyzed. In Auger electron spectroscopy, individual particles can be analyzed, but this type of analysis was not found to be useful because it was hampered by excessive charging of the samples because of their nonconductive nature. In addition, some particles were transferred to transmission electron microscopy grids that were covered with a carbon film to support the particles. In this case, individual samples could be analyzed, but those data will be presented in a future report because they are not yet summarized.

The XPS data show that the particles do not contain any metals and, in fact, have an atomic composition almost identical to that of the polycarbonate filter. We currently believe that this indicates that the particles are primarily soot-based and not formed from volatilization of metals in the FBG. The data indicate that the soot-based particles are not well burned in the thermal oxidizer, although they are significantly oxidized, nitrided, and sulfidized in the combustor. Ion etching to remove the surfaces of the particles indicate that the oxidation, nitridation, and sulfidation of the particles are primarily surface phenomena.

NOMENCLATURE

APMT®	oxide dispersion-strengthened FeCrAl alloy made by Kanthal
ASME	American Society of Mechanical Engineers
CM247LC	alumina-scale-forming nickel-based superalloy
CVAAS	cold-vapor atomic absorption spectrometry
EDS	energy-dispersive spectroscopy
EFG	entrained-flow gasifier
EPA	U.S. Environmental Protection Agency
FBG	fluid-bed gasifier
Rene® 80	alumina-scale-forming nickel-based superalloy
SEM	scanning electron microscopy
UTSR	University Turbine System Research

PREPARATION AND TESTING OF CORROSION- AND SPALLATION-RESISTANT COATINGS

INTRODUCTION

The objective of this Energy & Environmental Research Center (EERC) was to take a recently developed method of plating nickel superalloys with protective FeCrAl layers closer to commercial use in syngas-fired turbines. The project is designed to determine if plating APMT®, a specific highly oxidation-resistant oxide dispersion-strengthened FeCrAl alloy made by Kanthal, onto nickel-based superalloy turbine parts is a viable method for substantially improving the lifetimes and maximum use temperatures of the parts, both those with thermal barrier coatings (TBCs) and those without. The superalloys being investigated for protection are CM247LC and Rene® 80, both alumina-scale-forming alloys. The method for bonding the APMT plate to the superalloys is called evaporative metal bonding (EMB), which involves placing a thin foil of zinc (Zn) between the plate and the superalloy, clamping them together, and heating in an atmosphere-controlled furnace. Upon heating, the Zn melts and dissolves the oxide skins of the alloys at the bond line, allowing the two alloys to diffuse into each other. The Zn then diffuses through the alloys and evaporates from their surfaces.

If successful, the information developed will help move the protection process closer to demonstration testing. In addition, the team will characterize the microcontaminants in combusted higher-hydrogen-content gas. This information will be used to best simulate actual corrosion conditions in a turbine system and can also be used by other researchers studying deposition and gas flow in turbines.

EXPERIMENTAL METHODS

Laboratory Testing and Modeling

Under Tasks 2 and 3, we are measuring properties of the alloys and developing computer models of their high-temperature properties in order to develop the best methods for joining the APMT plate to CM247LC and Rene 80 turbine parts. In order to determine the best heating schedules to use for joining APMT plates to superalloy parts, we are measuring the diffusion rates of Zn through the alloys as a function of temperature. The experimental setup is described in last year's annual report. In order to develop the best clamp designs to use for holding the plating to the parts, we are measuring physical properties of the materials as a function of temperature.

Gasifier Sampling

In addition to the laboratory testing, we are continuing Task 4 sampling activities to determine what types of trace contaminants may occur in cleaned syngas that could lead to corrosion issues in turbines firing syngas. The EERC has several pilot-scale gasifiers that are continually used in a variety of test configurations. They are described in detail in last year's annual report. Funding for the actual operation of the gasifiers comes from projects other than

this University Turbine Systems Research (UTSR) project. The trace contaminants are collected using standard U.S. Environmental protection Agency (EPA) sampling techniques after the syngas produced by the gasifiers is burned in refractory-lined thermal oxidizers. The sampling trains used are for EPA Method (M) 29 sampling for particulate- and vapor-phase metals and M26A for halogens. Sampling is conducted when either one of two pilot-scale gasifiers are being operated. One is a pressurized entrained-flow gasifier (EFG), and the other is a pressurized fluid-bed gasifier (FBG).

RESULTS AND DISCUSSION

Laboratory Testing

Final analysis of the diffusion rates of zinc through the three alloys has been completed. After bonding, each joint was sectioned parallel to the sample axis (perpendicular to the bond line) and each joint analyzed via scanning electron microscopy (SEM) and energy-dispersive spectroscopy (EDS). EDS data were then used to estimate the diffusivity of zinc in each alloy at each temperature based on Equation 1 [1]:

$$C(x,t) = \frac{\beta}{2\sqrt{\pi D^* t}} exp\left(\frac{-x^2}{4D^* t}\right) \quad \text{[Eq. 1]}$$

where β is the initial concentration of diffusing species, D* is the diffusivity, t is time, and x is distance from the midline. Originally, it was planned that we would determine the diffusion rates at several different temperatures in order to determine bonding times at various temperatures. However, we have found that we were not able to create joints when temperatures much lower than the original temperature of 1214°C are used. Therefore, we limited our diffusion rate measurements to the two hold temperatures used in the procedure: 700° and 1214°C.

Table 1 shows diffusivity calculations for the APMT and CM247LC at 700°C. The units are given as volume/distance/time. No usable results were able to be obtained for the Rene 80 samples at this temperature. Table 2 shows the calculated diffusivities for APMT, CM247LC, and Rene 80 at 1214°C. In both tables, “Center” indicates composition data taken from the midline of the sectioned joints. “Edge” indicates composition data taken from the outer limit of the bonded region. This is illustrated in Figure 1. The apparent higher diffusion rate measured at the edge is greater than that at the center because the method is based on changes in composition with distance, and near the edges, zinc evaporates from the surface, creating a more rapid apparent diffusion rate.

Table 3 shows the center line composition of each of the joints from Tables 1 and 2 (data taken at the center position of each joint).

Several observations can be made about the data in Tables 1–3. First, the diffusivity of zinc in both APMT and CM247LC is quite similar at 700°C. Diffusivity in the APMT appears to be slightly higher (~4 vs. ~2 μm^2/min), but the midline composition after 30 minutes at this

Table 1. Calculated Diffusivities of Zinc in APMT and CM247LC at 700°C Based on EDS Data

Material	Temp., °C	Time, min	Center D, μm^2/min	Edge D, μm^2/min
APMT	700	30	3.29	4.10
CM247LC	700	30	1.23	1.81

Table 2. Calculated Diffusivities of Zinc in APMT, CM247LC, and Rene 80 at 1214°C Based on EDS Data

Material	Temp., °C	Time, min	Center D, μm^2/min	Edge D, μm^2/min
APMT	1214	60	103.57	142.58
	1214	300	130.82	N/A[1]
CM247LC	1214	60	5.33	15.66
	1214	180	8.55	7.13
	1214	300	3.71	3.75
	1214	600	5.87	N/A
	1214	1200	1.17	N/A
Rene 80	1214	60	15.64	9.37
	1214	180	9.66	8.79
	1214	300	8.31	6.96
	1214	600	3.00	N/A
	1214	1200	6.21	N/A

[1] Not analyzed.

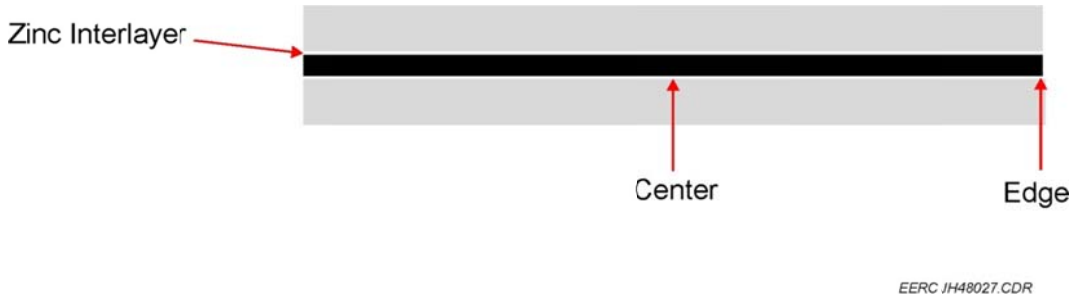

Figure 1. Schematic showing location of center and edge data.

temperature is quite similar. At 1214°C, the situation is very different. Because only about 15 wt% zinc remained at the midline after the low-temperature hold, the absolute difference in compositions between the APMT, CM247LC, and Rene 80 at 1214°C is relatively small. However, the calculated diffusivity of zinc in APMT is approximately 15 times higher than in CM247LC or Rene 80 (~120 vs. ~8 μm^2/min) at 1214°C. Equation 2 is the standard expression

Table 3. Center Line Composition of Each Joint, wt% zinc

Material	Temp., °C	Time, min	Center Composition, wt%
APMT	700	30	16.2
	1214	60	2.6
	1214	300	1.9
CM247LC	700	30	16.7
	1214	60	6.9
	1214	180	4.1
	1214	300	3.5
	1214	600	3.7
	1214	1200	2.1
Rene 80	1214	60	8.1
	1214	180	6.8
	1214	300	4.8
	1214	600	2.7
	1214	1200	1.4

for diffusivity in terms of the diffusion coefficient, Do, and the activation energy for diffusion, Q, where R is the ideal gas constant and T is the absolute temperature:

$$D^* = D_o exp\left(\frac{-Q}{RT}\right) \quad \text{[Eq. 2]}$$

If D_o and Q are assumed to be independent of temperature and composition for each material system and the approximate ratio of the diffusivities calculated above is substituted into Equation 2 for APMT and CM247LC, the difference in activation energies for diffusion of zinc through the two alloys can be estimated. This calculation yields:

$$Q_{CM247} - Q_{APMT} \cong -54 \frac{kJ}{kmol} \quad \text{[Eq. 3]}$$

For reference, this value is similar in magnitude and sign to the difference in activation energies for the diffusion of copper in pure nickel (258 kJ/kmol) and pure iron (295 kJ/kmol) [2].

Modeling

Table 4 shows the linear coefficient of thermal expansion as a function of temperature for each of the materials used in this study (parent materials and jig materials). Each value is the average of four measurements. The units are microstrain/°C, sometimes given as $x10^{-6}$/°C. These data were entered into a finite element model of the sample and jig to determine the stress distribution within the joint during bonding. The finite element model is shown in Figure 2. Figures 3–5 (units in Pa) show that the stresses at the bond line are not symmetrical about the axis of the joint during bonding. This is because of the geometry of the jig and the contact

Table 4. Linear Coefficient of Thermal Expansion (α) as a Function of Temperature for Each Material Involved with the Bonding Process

Temperature, °C	APMT, με/°C	CM247LC, με/°C	Rene 80, με/°C	Mo, με/°C	Steel, με/°C
100	13.51	12.49	12.74	7.51	16.03
200	14.91	13.64	14.18	8.51	18.13
300	17.14	14.83	15.17	10.02	20.59
400	18.54	15.65	15.93	10.94	21.86
500	19.28	16.24	16.42	11.49	22.61
600	19.54	16.70	16.76	11.67	23.04
700	19.99	17.12	17.17	11.90	23.19
800	20.15	17.44	17.50	12.08	21.92
900	20.49	17.74	17.98	12.13	22.23
1000	20.85	17.89	18.64	13.32	22.48
1100	21.21	17.53	19.63	14.70	22.68
1200	21.45	17.37	20.57	15.19	22.99

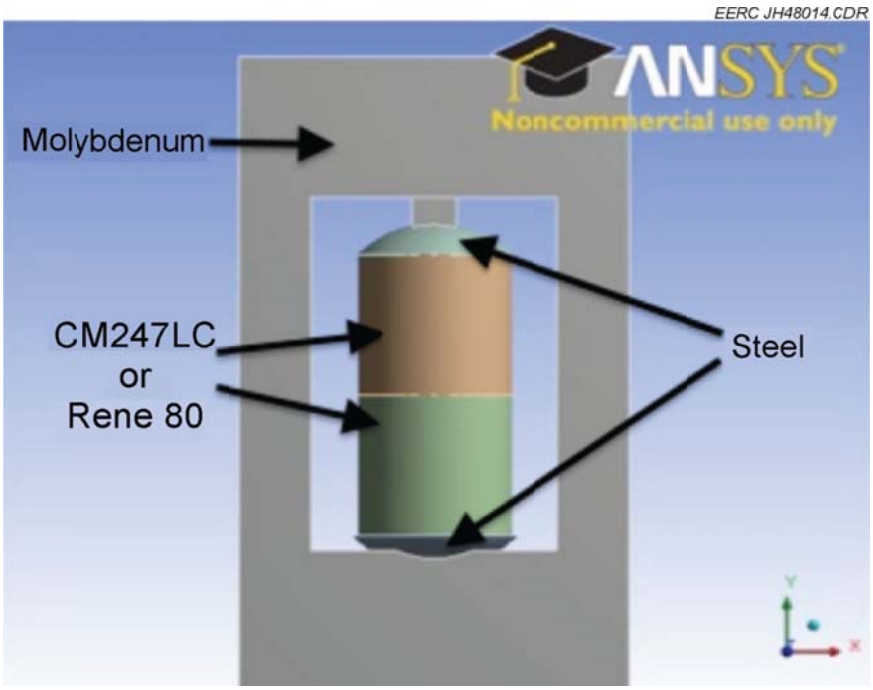

Figure 2. Finite element model used to study stress distributions during bonding.

between the jig and the steel hemispheres. Additional finite element simulations were conducted in which the boundary conditions on the outer edge of the steel spheres ranged from just the center point to the entire outer surface of the spheres. In general, the more tightly the steel spheres are constrained, the higher the value of effective stress at the bond line.

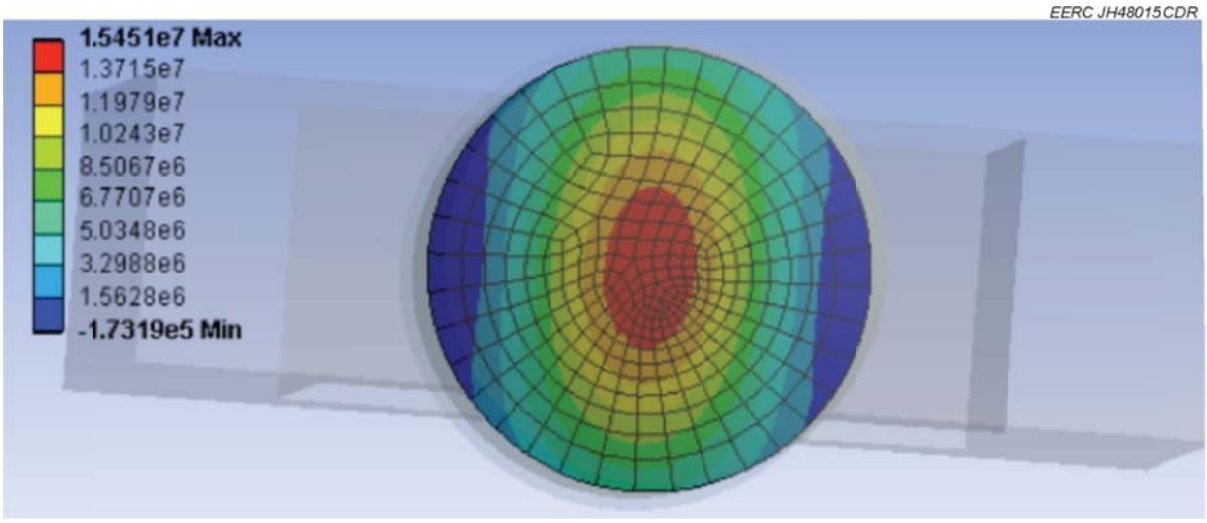

Figure 3. Normal stress distribution at the bonding interface during bonding of CM247LC.

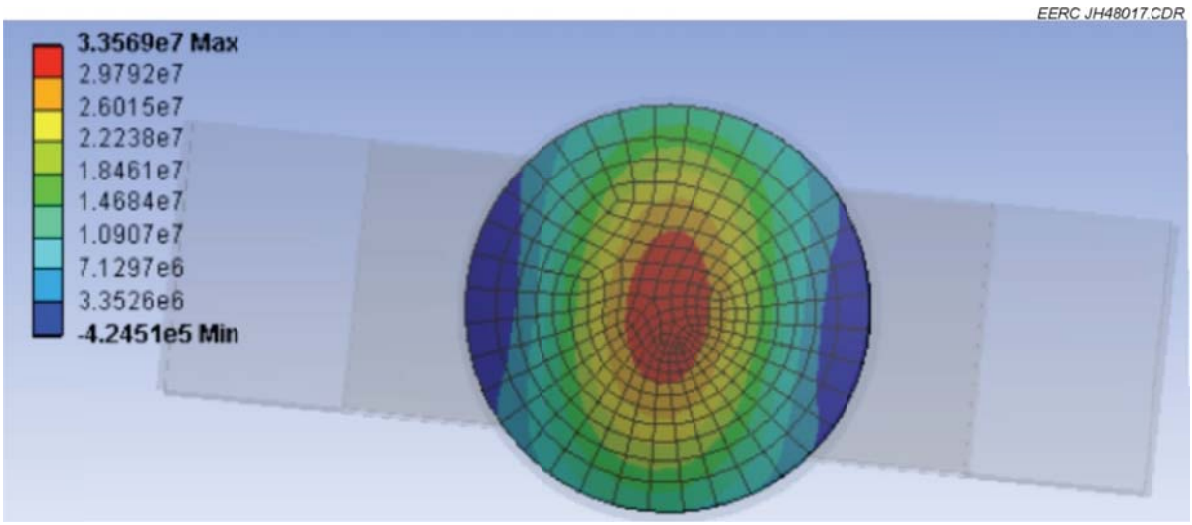

Figure 4. Normal stress distribution at the bonding interface during bonding of Rene 80.

Gasifier Sampling

In addition to the laboratory testing and modeling, Task 4 gasifier sampling activities continue to determine what types of trace contaminants may occur in cleaned syngas that could lead to corrosion or deposition in turbines firing coal syngas. The EERC has several pilot-scale gasifiers that are continually used in a variety of test configurations as determined by the needs of the projects that are funding the tests. Under the UTSR Program, we are sampling both noncombusted and combusted syngas produced during some of the pilot-scale gasifier tests. The pressurized EFG was described in the January–March 2012 quarterly report, and the pressurized FBG was described in the April–June 2012 quarterly report. The thermal oxidizer used to

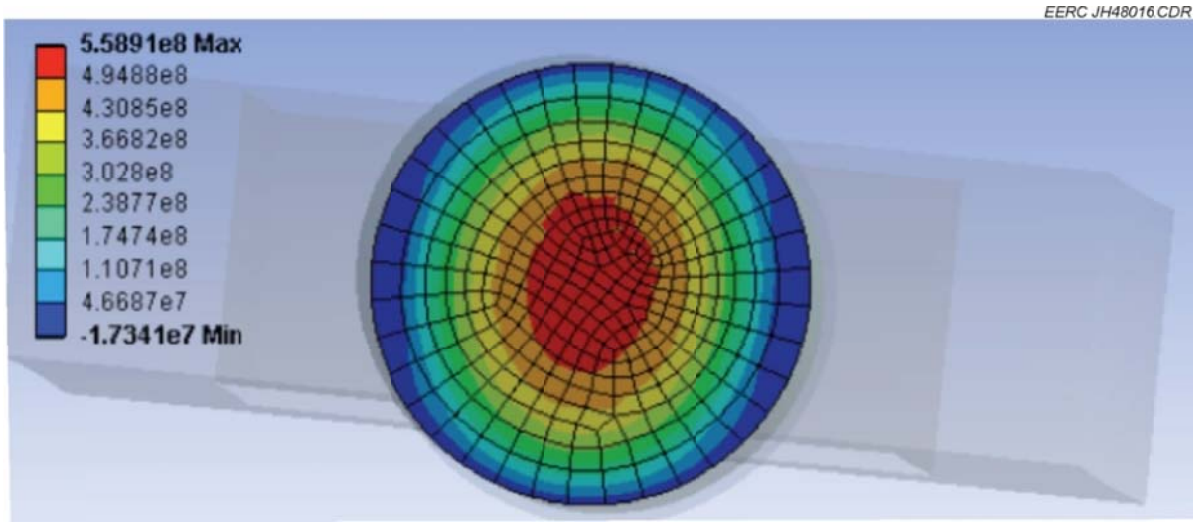

Figure 5. Normal stress distribution at the bonding interface during bonding of APMT.

combust the syngas contains a burner at the top of a refractory-lined chamber that admits the syngas and air separately and also includes a premixed natural gas and air supplemental gas stream. An accurate flame temperature is not available for the thermal oxidizer because thermocouples burn out too quickly in the flame. The sampling occurs both at the inlet and at the bottom of the downfired oxidizer. The gas being sampled is at approximately 750°C. It is quenched as it is pulled through the glass sampling tube to approximately 100°C before reaching the filter. The sampling train consists of a one-piece glass nozzle–probe liner, a large particulate cyclone, a polycarbonate filter (Whatman™ Nuclepore™ type with 0.1-µm holes), followed by a series of six impingers EPA M29. Impingers are of a standard Greenburg–Smith design type and are connected in series with leak-free, ground brass fittings.

The gas and particulate sample is withdrawn nonisokinetically from the source, particulate emissions are collected in the probe and on a heated filter, and gaseous emissions are then collected in aqueous acidic solutions of H_2O_2 and $KMnO_4$, respectively. While filters are analyzed using SEM, impinger solutions are analyzed using inductively coupled plasma–mass spectrometry. A target trace metal emission will be detected only if its concentration is above the corresponding lower limit of quantitation.

In M29, the first and second impingers contain 150 mL each of the mixture HNO_3–H_2O_2 (5% HNO_3 and 10% H_2O_2), the third impinger is empty, the fourth and fifth impingers both contain 150 mL of the mixture H_2SO_4–$KMnO_4$ (4% $KMnO_4$ and 10% H_2SO_4), and the sixth impinger contains about 350 g of preweighed silica gel. The HNO_3–H_2O_2 mixture is used to trap all of the heavy and trace metals (including the oxidized form of mercury) that have gone through the filter's pores, while the H_2SO_4–$KMnO_4$ mixture is used to trap the elemental form of mercury.

Before sampling, a pretest leak check is conducted, and the initial meter volume is recorded. For each run, the required data are recorded on a data sheet. At the end, the glassware is disconnected, and the contents of the acid impingers are poured into a leak-free storage bottle.

Each impinger is rinsed with water, and the rinse is added to the corresponding storage bottle. All sample collection bottles are sealed, labeled, and sent to the analytical laboratory for analysis.

During the January to March 2013 quarterly reporting period, sampling was performed at both the inlet and the outlet of the thermal oxidizer while the pressurized FBG was firing a subbituminous coal from the Eagle Butte Mine, Wyoming. No sulfur removal technology was used during the gasifier test. Four M29 samples were collected, two immediately before the thermal oxidizer and two at the bottom of the thermal oxidizer. The first test was conducted on March 12 (Test 1), the second (Test 2) and third on March 13 (Test 3), and the fourth test on March 15 (Test 4). The first and second tests were conducted at the inlet before the combustor, while the third and fourth tests were conducted at the outlet after combustion.

During the March to June 2013 quarterly reporting period, we attempted to analyze these filter samples in the EERC JEOL 5800 SEM equipped with an Oxford Instruments INCA EDS system and a silicon drift x-ray detector. However, measureable x-ray signals could not be obtained with the EERC EDS system, so the compositions of the particles could not be determined. Therefore, during the current reporting period, a piece of the filter sample collected from the inlet to the thermal oxidizer was sent to JEOL USA for analysis by Natasha Erdman with a more powerful field emission-type SEM.

Figure 6 shows an image of the inlet particles with the JEOL USA system. The particles captured at the inlet have diameters typically between 0.2 and 0.5 µm. Figure 7 is composed of two higher-magnification images of the same area. Figure 7a is taken using secondary electron imaging (SEI), whereas 2b is taken using backscatter electron imaging (BEI). In BEI imaging, the contrast is modified by the density of the particles, denser particles appearing brighter than less dense particles. The images show that a few of the particles are denser than the majority of the particles and, therefore, likely contain higher-atomic-number elements such as sulfur or metals. It also shows that many of the larger particles are composed of conglomerates of 0.1-µm particles. However, JEOL USA was also not able to obtain sufficient EDS data from the small particles for identification, other than carbon and sulfur, which could have been interference from x-rays emanating from the underlying filter. The small black circles are holes in the filter.

Figure 8 is an SEI image taken with the EERC SEM showing particles collected on the filter at the outlet of the thermal oxidizer. The image shows that the particles are somewhat larger and more spherical than those at the inlet to the oxidizer. As with the inlet particles, the EDS data were not conclusive as to the compositions of these particles, although more oxygen was detected.

Figure 9 is an SEI image taken with the EERC SEM showing particles collected on the filter at the outlet of the thermal oxidizer when no syngas was being burned in the oxidizer. It shows that the particles collected are much smaller and much less concentrated than the filter samples collected from the syngas and from the syngas combustor.

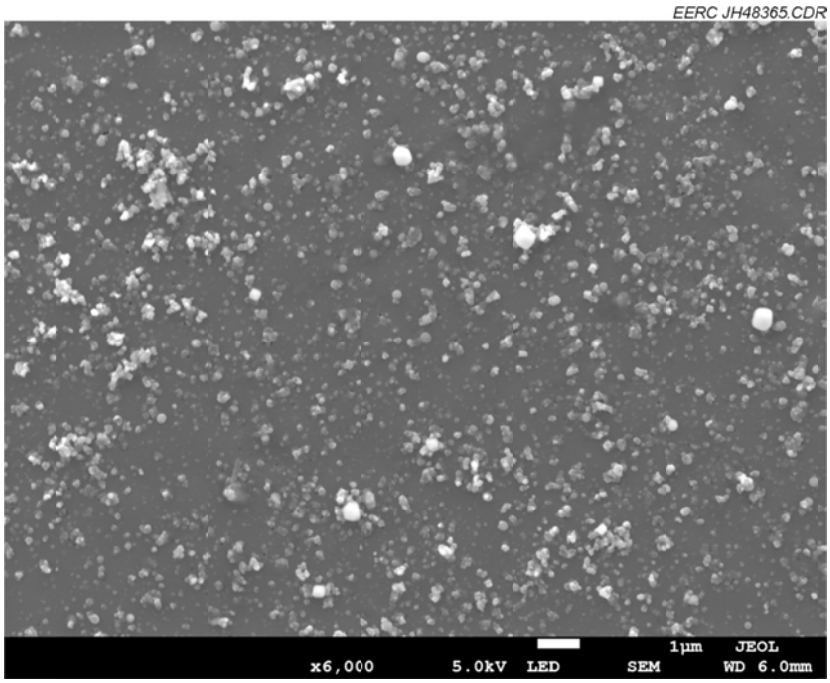

Figure 6. SEI image of particles collected on the filter at the thermal oxidizer inlet.

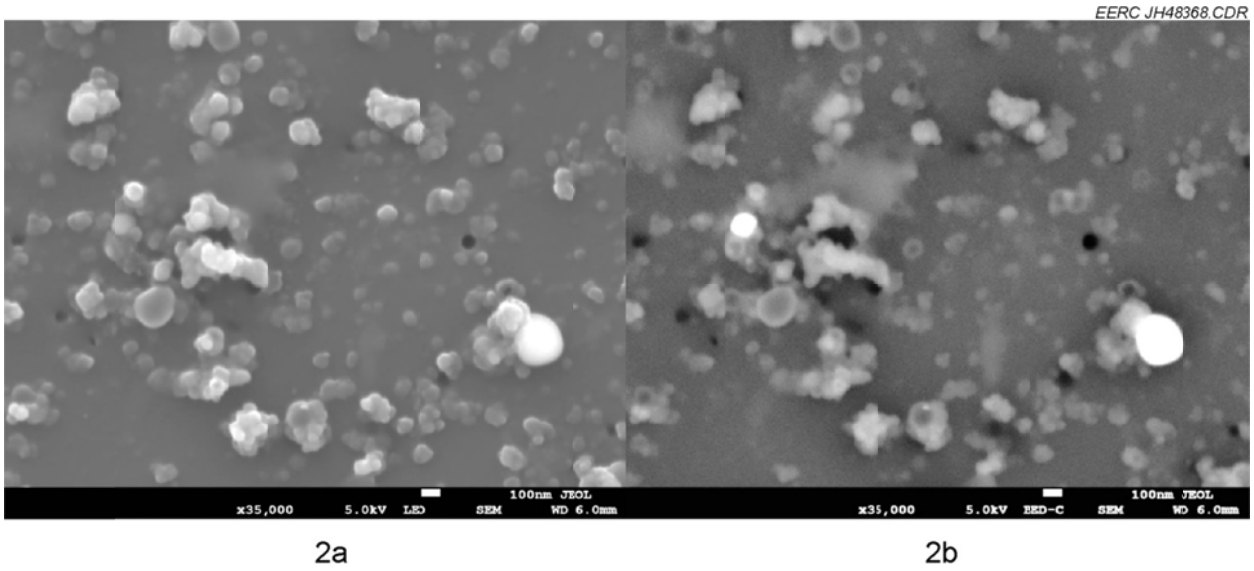

Figure 7. Higher-magnification views of the same area showing the differences between SEI (2a) and BEI (2b) images.

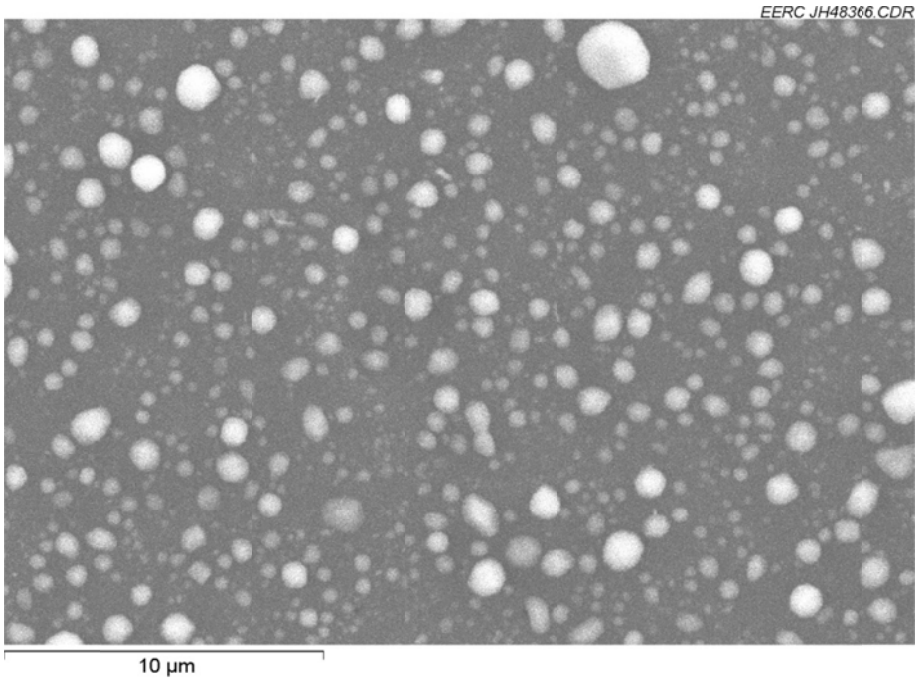

Figure 8. SEI image of particles collected on the filter at the thermal oxidizer outlet.

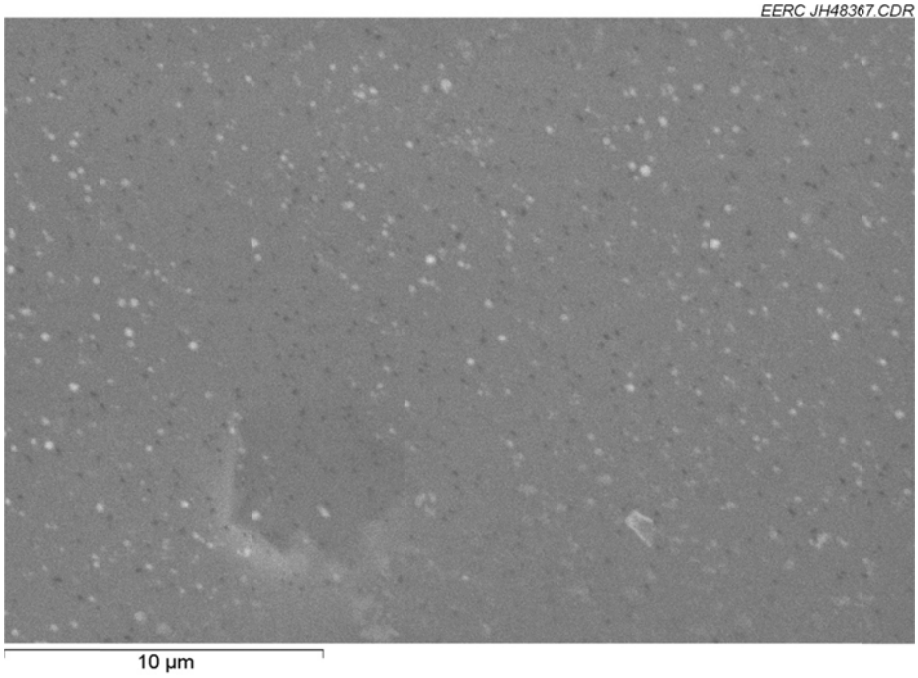

Figure 9. SEI image of particles collected on the filter at the thermal oxidizer inlet when no syngas was being burned.

Because the EDS signals collected for the particles both at the EERC and JEOL USA were not conclusive as to the compositions of the particles collected on the filters, the EERC applied for time on electron microscopes using different signal analyzers at the Oak Ridge National Laboratory (ORNL) ShaRE User Facility, which is sponsored by the U.S. Department of Energy Scientific User Facilities Division of the Office of Basic Energy Sciences. The analyses were performed by Karren More and Henry Meyer III. At ORNL, both x-ray photoelectron spectroscopy (XPS) and Auger electron spectroscopy were performed on the samples because these are surface analyses that analyze electrons emitted from within a few nanometers of the surfaces of the particles and filters. In XPS, areas of the filter on which particles reside are analyzed. In Auger electron spectroscopy, individual particles can be analyzed, but this type of analysis was not found to be useful because it was hampered by excessive charging of the samples because of their nonconductive nature. In addition, some particles were transferred to transmission electron microscopy grids that were covered with a carbon film to support the particles. In this case, individual samples could be analyzed, but those data will be presented in a future report because they are not yet summarized.

Figures 10–17 show summaries of the findings of the XPS analyses. In Figure 10, the electron spectrum for the thermal oxidizer inlet sample containing both particles collected from the unburned syngas and filter area is compared to the spectrum for just the filter. The data show that the particles do not contain any metals and, in fact, have an atomic composition almost identical to that of the polycarbonate filter. We currently believe that this indicates that the

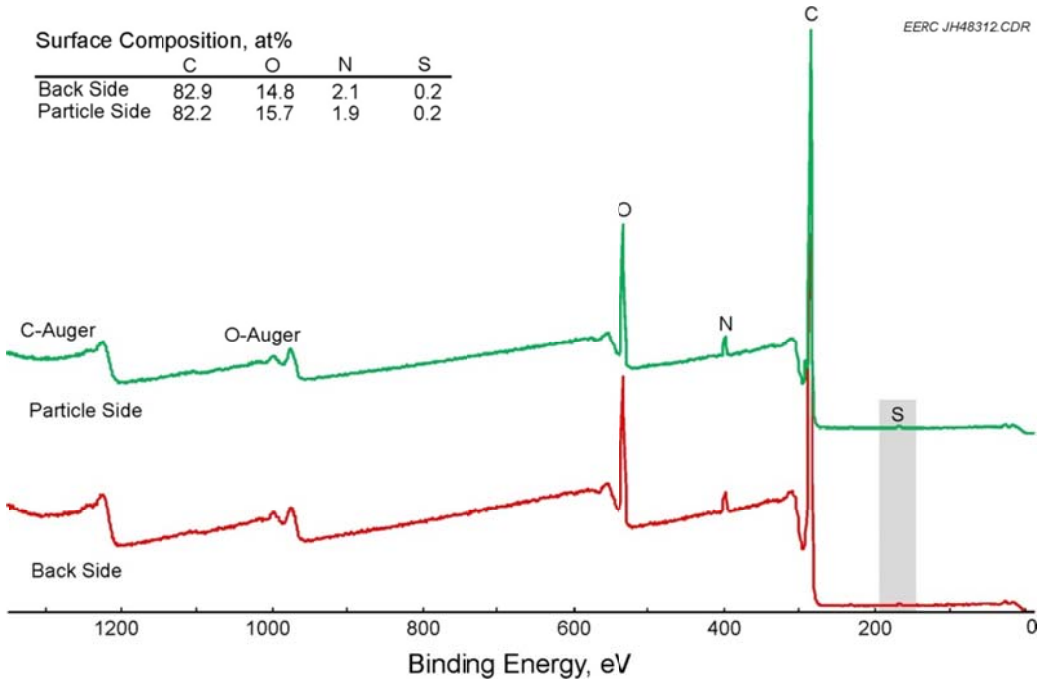

Figure 10. XPS spectrum for an area on the front side (filter + particles) of the filter sample collected from the inlet to the thermal oxidizer on March 13, 2013, compared to the spectrum collected from an area on the back side (just filter material).

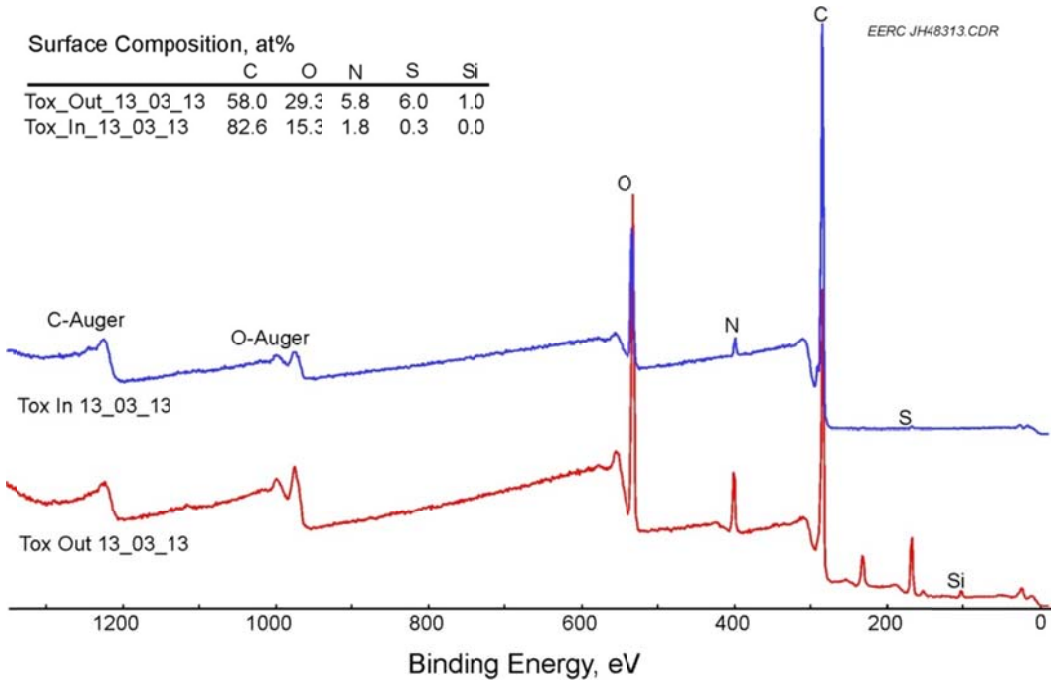

Figure 11. XPS spectra for an area of the filter covered with particles collected from the inlet of the thermal oxidizer (blue) compared to an area of the filter covered with particles collected from the outlet of the thermal oxidizer (red).

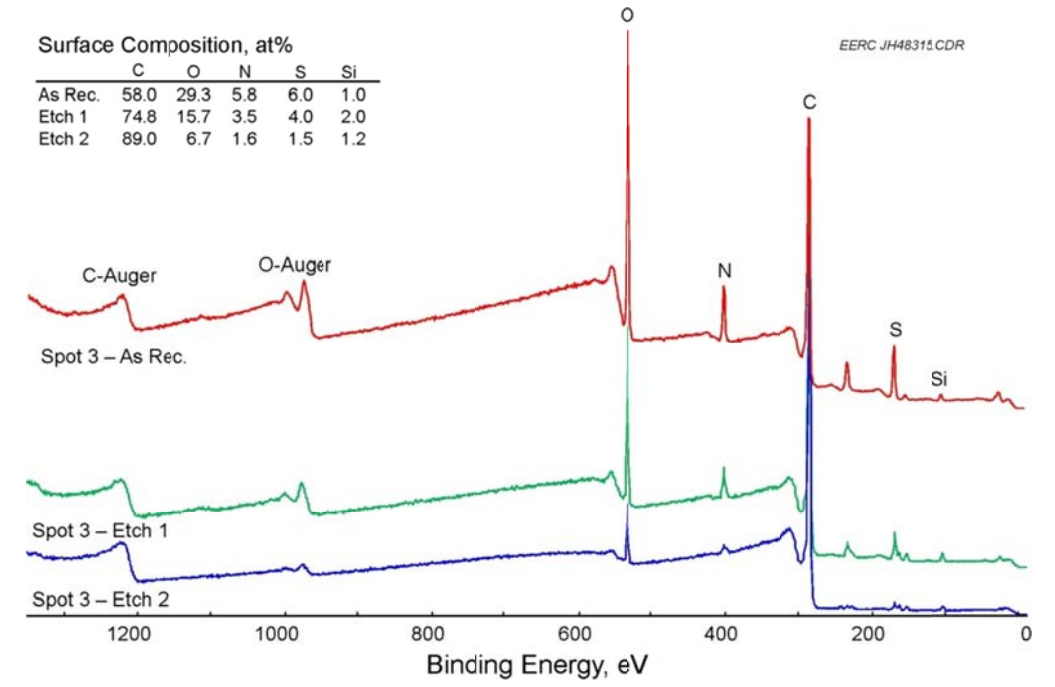

Figure 12. XPS spectra for an area of the filter covered with particles collected from the outlet of the thermal oxidizer before ion etching (red) and after one (green) and two (blue) etching cycles.

particles are primarily soot-based and not formed from volatilization of metals in the FBG. Figure 6 compares the spectra for particles collected from the syngas to the particles collected from the combusted syngas. Filter area is also included in the analyses. The data indicate that the soot-based particles are not well burned in the thermal oxidizer, although they are significantly oxidized, nitrided, and sulfidized in the combustor.

Figure 7 shows data for the thermal oxidizer outlet particles as well as spectra for the same areas after one and two ion etchings. The etching removes the outer layers of the particles. The data indicate that the oxidation, nitridation, and sulfidation of the particles are primarily surface phenomena.

CONCLUSIONS

We have found that we were not able to create joints when temperatures much lower than the original temperature of 1214°C are used. Therefore, we limited our diffusion rate measurements to the two hold temperatures used in the procedure: 700° and 1214°C. The diffusivity of zinc in both APMT and CM247LC is quite similar at 700°C. Diffusivity in the APMT appears to be slightly higher, but the midline composition after 30 minutes at this temperature is quite similar. At 1214°C, the situation is very different. The calculated diffusivity of zinc in APMT is approximately 15 times higher than in CM247LC or Rene 80 (~120 vs. ~8 μm^2/min) at that temperature.

In addition to the diffusion work, the coefficients of thermal expansions were determined for each of the alloys as a function of temperature. This information has been entered into a finite element model using ANSYS so that appropriate force-applying structures can be designed for use in joining structures composed of APMT and the nickel alloys.

Gasifier sampling activities continue to determine what types of trace contaminants may occur in cleaned syngas that could lead to corrosion or deposition in turbines firing coal syngas. The EERC has several pilot-scale gasifiers that are continually used in a variety of test configurations as determined by the needs of the projects that are funding the tests. We are sampling both noncombusted and combusted syngas produced during some of the pilot-scale gasifier tests.

SEM analyses showed that the particles captured on the filter from the syngas were typically 0.2 to 0.5 μm in diameter, whereas those captured from the combusted syngas were slightly larger and more spherical. However, the particles were so small that we could not obtain good spectra from them either at the EERC or JEOL America. At ORNL, XPS data show that the particles do not contain any metals and, in fact, have an atomic composition almost identical to that of the polycarbonate filter. We currently believe that this indicates that the particles are primarily soot-based and not formed from volatilization of metals in the FBG. The data indicate that the soot-based particles are not well burned in the thermal oxidizer, although they are significantly oxidized, nitrided, and sulfidized in the combustor. Ion etching to remove the surfaces of the particles indicates that the oxidation, nitridation, and sulfidation of the particles are primarily surface phenomena.

REFERENCES

1. Poirier, D.R.; Geiger, G.H. *Transport Phenomena in Materials Processing*; TMS, Warrendale, PA, 1994.

2. Butrymowicz, D.B.; Manning, J.R.; Read, M.E. Diffusion in Copper and Copper Alloys Part IV. Diffusion in Systems Involving Elements of Group VIII. *J. Phys. Chem. Ref. Data* 1976, *5* (1), 103–200.

3. Hosford, W.H. *Mechanical Behavior of Materials*; Cambridge University Press: New York, 2006; p. 86.